REGULAR ARTICLE

Reactivity of H_2O and the Si-terminated surface of silicon carbide studied with ONIOM method

Yan Liu · Ke-He Su · Qing-Feng Zeng ·
Lai-Fei Cheng · Li-Tong Zhang

Abstract The reactivity of H_2O and the Si-terminated silicon carbide surface (001) was investigated on the triplet potential energy surface with the combined first principle and molecular mechanics ONIOM(CASSCF:AM1:UFF) method for the $(SiC)_{192} \cdot H_2O$ model. It was found that the H_2O molecule and the surface can form three physisorption complexes and follow five reaction paths to produce eight products, in which there are five main products having necessary energy barriers less than 300 kJ mol^{-1}. Compared with that on the C-terminated surface, the interaction with the Si-terminated surface has stronger physisorption energy, smaller lowest necessary energy barrier, more main and more stable products.

Keywords SiC · H_2O · Reactivity · ONIOM

1 Introduction

In the previous paper [1], the oxidation mechanisms and reaction paths of a H_2O molecule on the C-terminated

Y. Liu · K.-H. Su (✉)
Key Laboratory of Space Applied Physics and Chemistry
of the Ministry of Education, School of Natural and Applied
Sciences, Northwestern Polytechnical University, Xi'an 710072,
Shaanxi, People's Republic of China
e-mail: sukehe@nwpu.edu.cn

Y. Liu
College of Chemistry and Life Science,
Weinan Normal University, Weinan 714000,
Shaanxi, People's Republic of China

Q.-F. Zeng · L.-F. Cheng · L.-T. Zhang
National Key Laboratory of Thermostructure Composite
Materials, Northwestern Polytechnical University,
Xi'an 710072, Shaanxi, People's Republic of China

(001) silicon carbide surface were investigated with ONIOM(B3PW91/6-31g(d):AM1:UFF) method. However, Cicero et al. [2, 3] found that the water dissociation on the C-terminated surface is hydrophobic characterized, while that on the Si-terminated is hydrophilic with spontaneous reactions by means of ab initio molecular dynamics simulations with generalized gradient approximations. The structure and the dissociation energies of the H_2O molecule on the surfaces were reported, but the associated dissociation transition states or reaction paths were not covered. Therefore, the present work is further carried out to demonstrate the insights of the reactivity of a water molecule with the Si-terminated surface.

Actually, the research for the oxidation of silicon carbide surface has attracted much attention as one of the most important concerns in experiments [4–18]. It is also found that water is the most commonly encountered oxidant that would accelerate significantly the oxidation of SiC [6, 17, 19–25]. Hydroxides of silicon have been observed as the products of the SiC surface water dissociations [22–25]. However, the detail information of the reactions (i.e., the structures and energies of the adsorbents, intermediates, transition states as well as the reaction pathways) still remains unknown that needs to be investigated and compared with that on the C-terminated surface [1].

2 Methodology and models

The model, as shown in Fig. 1a, is similar to that in [1], where there are 387 atoms involving 192 C, 192 Si atoms and a H_2O molecule in a slab of 12 layers of SiC and the water molecule is reacting with the Si-terminated surface. This model is about $1.65 \times 1.65 \times 1.23$ nm in dimension. The theoretical method, a three-layered ONIOM approach

[26–28], employed in this work is, however, different from that in [1]. This is because that the Si-terminated surface is typically of diradical nature [29] and our test calculations did result in lower energies for triplet states compared with singlets over all of the reactants, intermediates and products and with quintet state for the reactants and some intermediates. The theoretical layers are shown in Fig. 1b where the active region (represented by balls, involving 9 atoms $H_2O \cdot C_2Si_4$) is treated with the complete active space self-consistent field (CASSCF) method [30–35], the intermediate region (represented by thick sticks, involving 9 atoms C_6Si_3) is treated with the semi-empirical AM1 model [36–38], and the framework environment (represented by thin lines) is treated with the molecular mechanics (MM) by using the universal force field (UFF) [39]. The total energies of the ONIOM3 system within the framework of the ONIOM methodology developed by Morokuma et al. [40] can be expressed as

$$E_{ONIOM3} = E_{Low}^{Real} + \left(E_{Medium}^{Intermediate} - E_{Low}^{Intermediate}\right) + \left(E_{High}^{Model} - E_{Medium}^{Model}\right)$$

where the superscripts *Real, Intermediate and Model* denote the whole system, the intermediate layer and the active site region, respectively. Subscripts *Low, Medium and High* represent the low-, medium- and high-level methodologies in the ONIOM calculations. Since the diradical is an open-shell system and most of the reaction intermediates and transition states may have dramatic non-dynamic electronic correlations, the high-level method is chosen with the multi-referenced (CASSCF) method, where all the geometries are optimized with CASSCF(5,4)/6-31G(d) and the energies are refined with CASSCF(5,5)/6-311G(d,p), where the active spaces were chosen with 5 (an extra electron has to be involved due to the high-medium connection in the ONIOM approaches) active electrons allocated in 4 (former) and 5 (latter) active

orbitals. The geometries of the models are optimized with full degrees of freedom and characterized as either a minimum (no imaginary frequency) or a first-order saddle point (solely an imaginary frequency). The connection of the TS and the associated reactant and product is confirmed with the intrinsic reaction coordinates. All calculations are performed with the GAUSSIAN-09 packages [41].

3 Results and discussions

The optimized structure shows that the environment treated with MM/UFF remained almost unchanged compared with the bulk structure. The Si–C bond distances are within 0.186–0.197 nm, which are consistent with the experimental value 0.189 nm in the crystalline [42]. The Si–C distances from the semi-empirical AM1 are within 0.184–0.192 nm, and those reproduced by CASSCF(5,4)/6-31g(d) for the active region are within 0.181–0.193 nm. The outermost silicon atoms reconstruct with the Si–Si distances at about 0.24 nm due to their unsaturated chemical environment on the surface, which reflects well the surface reconstructions of the experimental LEED value 0.231 nm [43] and is consistent with the theoretical value 0.246 nm of [29]. Therefore, the model and the theoretical method simulated well the actual structure of the Si-SiC surface.

The reactants, H_2O and the Si-terminated SiC(001) surface model, were combined by physically placing the H_2O molecule 1.0 nm away from the optimized Si-SiC surface to calculate the total energy (also in triplet state) of the reactants in eliminating the errors of the inconsistency of the systems. For example, the energy of a pure CASSCF of a free H_2O plus a pure ONIOM Si-SiC model is not equal to that of the combined (but almost interaction-free) system since the pure energy of the H_2O molecule has not
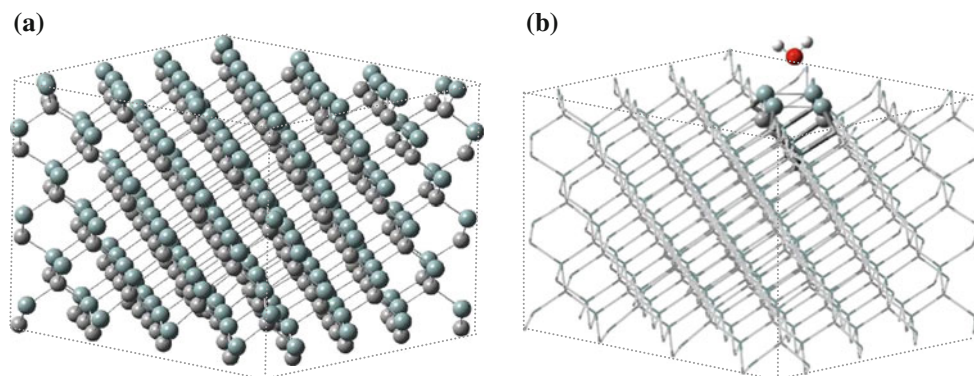

Fig. 1 Structure and the ONIOM layers of the model employed in this work. **a** Bulk model of the Si-terminated SiC(001) surface. **b** Outline of the ONIOM3 theoretical layers for the H_2O interacting Si-terminated SiC(001) surface (the *balls* represent the high layer, the *thick sticks* represent the medium layer, and the *thin lines* represent the low layer)

been involved in the E_{ONIOM} calculations as shown in the energy calculation equation. This treatment also applies for a product P4 + H$_2$.

The geometries of the intermediates, transition states and the products optimized with ONIOM(CASSCF(5,4)/6-31G(d):AM1:UFF) are shown in Fig. 2. The electronic energy (E), zero-point energy (ZPE), energy at zero Kelvin ($U_{0K} = E + ZPE$) and the relative energy (U_R) for each of the species as well as the dominant configuration coefficients are listed in Table 1. The profiles of the potential energy surface obtained with ONIOM(CASSCF(5,5)/6-311G(d,p):AM1:UFF) energy plus ZPE are schematically shown in Fig. 3.

3.1 Formation of the molecular complexes

Three molecular complexes IM1, IM2 and IM3 are found for a water molecule to be absorbed on the Si-terminated (001) surface of SiC as shown in Fig. 2. Since all the energies and the structures have not significantly changed, these complexes as well as the associated transition states were recognized as the species of physisorption. For example, the geometry of the water molecule (0.095 nm and 105.4°) in complex IM1 is almost unchanged compared with its gas phase structure. In IM1, the plane of the water molecule is almost parallel to the Si surface with the oxygen atom placed above the center of the active region. The distance from the oxygen atom to the nearest surface silicon atom is 0.3732 nm, which is about 0.04 nm longer than that on the C-terminated surface [1] due to the larger radius (also larger by 0.04 nm) of Si atom. Such distances should be large enough not to prevent significantly the surface from reconstruction. As shown in Fig. 3, the initial association of forming IM1 is a barrierless process. However, the adsorption energy 54.4 kJ mol^{-1} of IM1 is larger than that (25.1 kJ mol^{-1}) on the C-terminated surface [1]. This should be mainly from an additional interaction of the water molecule with the surface Si atoms. Actually, a natural orbital analysis [44, 45] shows that the lone pair electrons (as an electron donor) of the O atom in the H$_2$O molecule have some interactions with the empty 3d orbitals (as electron acceptors) of the four nearest Si atoms on the surface. This is consistent with the estimation of [2].

IM1 may transform into an absorbed state IM2 via transition state TS1 with a very small energy barrier of 10.0 kJ mol^{-1}. In IM2, the Si–O distance is 0.2050 nm, smaller than that in IM1 and the O atom is placed nearly at the top of a surface Si atom. The transition of TS1 into IM2 is also accompanied by the rotation of the H$_2$O molecule around the O–Si axis. Since the energy of IM2 is higher than TS1, more intermediates and transition states for the rotation must be existed. However, to our efforts so far, these species have not been found. IM2 may further transform into another slightly more stable complex IM3 via TS2 with an, also rotational, energy barrier of 13.3 kJ mol^{-1}. The adsorption energy of IM3 is −16.5 kJ mol^{-1}, which is 13.9 kJ mol^{-1} lower than that of IM2. The energy change from IM2 to IM3 via TS2 could be explained by the decrease of the positive charge repulsion between the Si and the H atoms during the H$_2$O rotation around the same O–Si bond. However, the O–Si bond in IM3 is slightly larger by 0.0086 nm than that in IM2, reflecting the complexity of the interactions.

3.2 Reaction pathways

Starting from complex IM3, five dissociation reaction channels (path1-5) are found as shown in Fig. 3, which involves 11 transition states (TS3-13) and 8 products (P1-8). Among these paths, path 1 is a single-step reaction and paths 2–5 are multi-step reactions. The details are discussed as follows.

The main feature of the reactions of IM3 is that the H$_2$O molecule breaks a O–H bond into two fragments (–H and –OH), and the hydrogen atom is absorbed on a surface Si atom, while the –OH group bonds onto another surface Si atom. Three possible dissociation products were obtained for different positions of the –H and –OH groups as shown by P1, P2 and P3 in Fig. 3. The corresponding transition states for these paths are TS3, TS4 and TS5, in which all the absorbed H atoms are more close to the surface Si atoms (i.e., 0.1887 nm in TS3, 0.2108 nm in TS4 and 0.1964 nm in TS5). The distances between Si and O decrease into 0.1743, 0.1803 and 0.1801 nm, while the breaking O–H bond lengths increase into 0.1378, 0.1139 and 0.1228 nm, respectively. The respective energy barriers are 102.6, 148.6 and 243.9 kJ mol^{-1}, and the reaction energies are −281.2, −303.8 and −256.6 kJ mol^{-1} with respect to IM3. The reaction energies with respect to the reactants are −297.7, −320.3 and −273.1 kJ mol^{-1}, and the magnitude consists very well with those ($\sim$300 kJ mol^{-1}) obtained in [2, 3] for the reactions in producing similar configured products. Obviously, the reaction via TS3 has the lowest energy barrier, but the H$_2$O molecule is not breaking the π bond within the Si dimer as shown by the structure of TS3 in Fig. 2. Instead, the O–H group is bridging two Si atoms within different dimmers. In the dissociation products P1, P2 and P3, the lengths of the Si–O bonds are 0.1656, 0.1661 and 0.1661 nm and those of the Si–H bonds are 0.1475, 0.1484 and 0.1482 nm, respectively. It is notable that P2 and P3 have the similar Si–O and Si–H bond lengths and the ab initio molecular dynamics also resulted in the similar structures (0.166 nm for Si–O bond and 0.149 nm for Si–H bond) [2, 3]. Actually, product P2 may convert into P3 via TS6 by swing the O–H bond around the Si–O axis with an energy barrier of 140.4 kJ mol^{-1} (and that is 93.2 kJ mol^{-1}
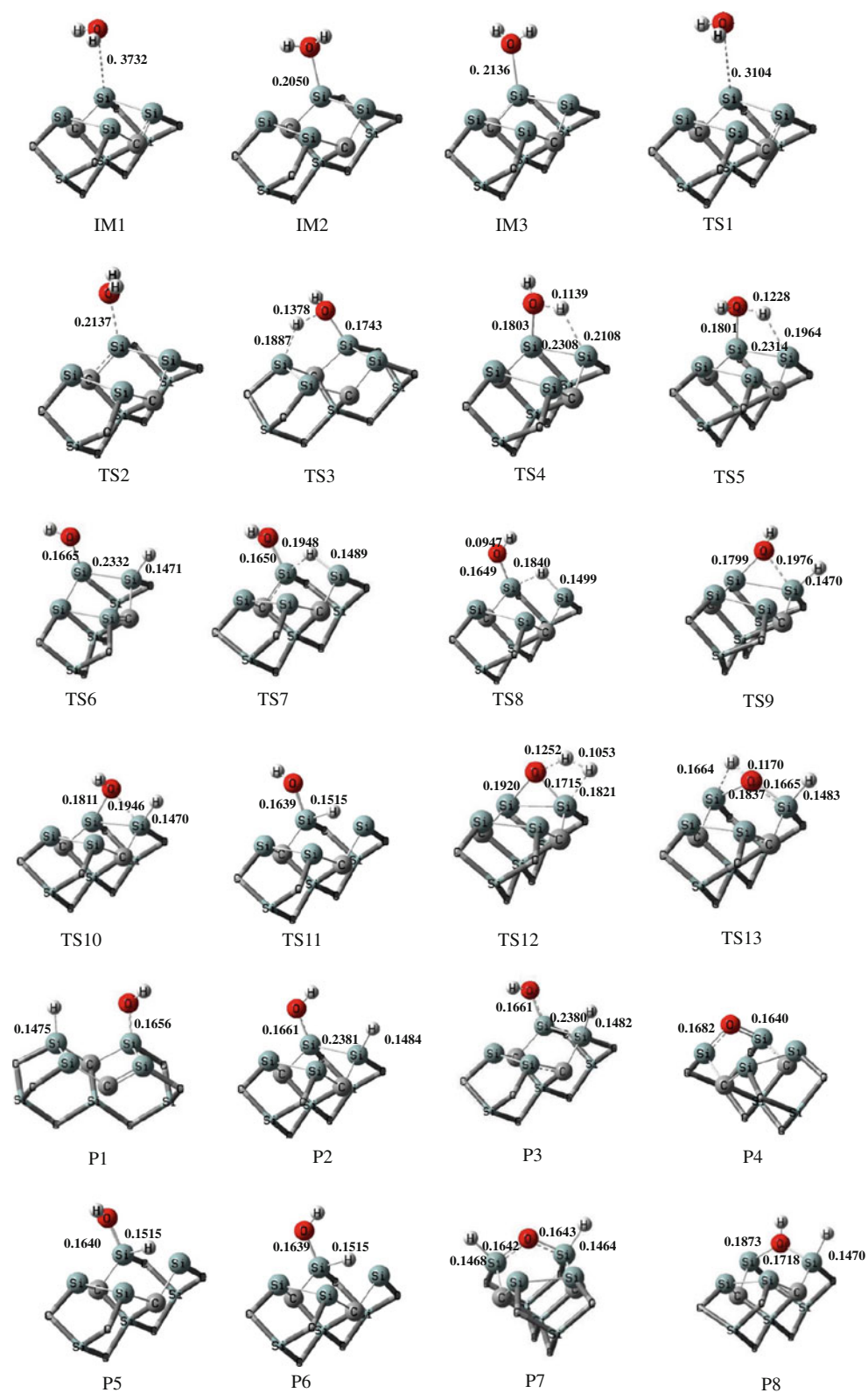
Fig. 2 Geometries of the intermediates, transition states and products optimized with ONIOM(CASSCF(5,4)/6-31G(d):AM1:UFF). All the species are in triplet states. Bond distances are in nanometers. Geometries of the environment are not shown in the figure

Table 1 Electronic energies (E), zero-point energies (ZPE), energies ($U_{0\ K}$) and the relative energies (U_R) of the reactants, intermediates, products, transition states as well as the dominant configuration coefficients obtained with ONIOM(CASSCF(5,5)/6-311G(d,p):AM1:UFF)// ONIOM(CASSCF(5,4)/6-31G(d):AM1:UFF)

Species (state)	Dominant configuration coefficients	E/a.u.	ZPE/a.u.	$U_{0\ K}$/a.u.	U_R/kJ mol^{-1}
SiC(^{3}A) + H$_2$O	0.92411	−1,312.537352	1.763207	−1,310.774145	0.0
IM1	0.92948	−1,312.543167	1.748303	−1,310.794864	−54.4
IM2	0.98424	−1,312.529634	1.754500	−1,310.775134	−2.6
IM3	0.97821	−1,312.530419	1.750001	−1,310.780418	−16.5
TS1	0.92817	−1,312.538060	1.746999	−1,310.791061	−44.4
TS2	0.98032	−1,312.529156	1.759097	−1,310.770059	10.7
TS3	0.99507	−1,312.509486	1.768141	−1,310.741345	86.1
TS4	0.98535	−1,312.470697	1.746853	−1,310.723844	132.1
TS5	0.98322	−1,312.485324	1.797781	−1,310.687543	227.4
TS6	0.99517	−1,312.626143	1.783494	−1,310.842649	−179.9
TS7	0.96923	−1,312.560664	1.794766	−1,310.765898	21.7
TS8	0.97705	−1,312.539728	1.754497	−1,310.785231	−29.1
TS9	0.97278	−1,312.516297	1.750562	−1,310.765735	22.1
TS10	0.97416	−1,312.518804	1.819323	−1,310.699481	196.0
TS11	0.98190	−1,312.563926	1.792295	−1,310.771631	6.6
TS12	0.99601	−1,312.394178	1.750224	−1,310.643954	341.8
TS13	0.98248	−1,312.528700	1.756983	−1,310.771717	6.4
P1	0.99528	−1,312.643626	1.756077	−1,310.887549	−297.7
P2	0.99490	−1,312.645270	1.749118	−1,310.896152	−320.3
P3	0.99993	−1,312.629193	1.751037	−1,310.878156	−273.1
P4 + H$_2$	0.94323	−1,312.582199	1.739078	−1,310.843121	−181.1
P5	0.98186	−1,312.568923	1.764310	−1310.804613	−80.0
P6	0.98243	−1,312.569982	1.753358	−1,310.816624	−111.5
P7	0.99996	−1,312.671706	1.752183	−1,310.919523	−381.7
P8	0.98022	−1,312.580481	1.772697	−1,310.807784	−88.3

for the reverse process). Therefore, P3 can be produced from P2 via TS6 with the smaller barrier of 140.4 kJ mol^{-1}.

It should be especially noted that the present work resulted in energy barriers for water molecule dissociating on the Si-SiC surface while [2, 3] proposed 'spontaneous' dissociations. Although the structure variations and the reaction energies are similar, the disagreement remains unknown that must be an interesting topic for further study either experimentally or theoretically.

P5 and P6, another pair of *cis–trans* isomers as shown in Fig. 2, may be obtained from the respective isomers P3 and P2 via TS7 and TS8 by 1,2-hydrogen shift processes with the energy barriers of 300.2 and 291.2 kJ mol^{-1}. The migrating H atom in the transition states is 0.1489 and 0.1499 nm away from the original Si atom that it connects and the distances of the forming Si–H bond are 0.1948 and 0.1840 nm. In P5 and P6, the Si–O bond lengths 0.1640 and 0.1639 nm are very close to each other and both of the Si–H bond lengths are 0.1515 nm. The *cis–trans* isomerization of P5 and P6 has an energy barrier of 86.6 (P5–P6)

or 118.1 kJ mol^{-1} (P6–P5) via TS11. Therefore, P5 can be produced from P6 via TS11 with the smaller barrier of 118.1 kJ mol^{-1}.

Products P2 and P3 may further isomerize into a same product P8 via TS9 and TS10 with higher energy barriers of 342.4 and 469.1 kJ mol^{-1}. The –OH group in P8 links two adjacent Si atoms and forms the bridge-bonded hydroxyl structure, in which the HOSiSi plane is almost perpendicular to the Si surface. The Si–O bond lengths are 0.1873 and 0.1718 nm, and the Si–H bond length is 0.1470 nm. These reactions are endothermic by 232.0 and 184.8 kJ mol^{-1}.

Product P8 would dissociate a molecular hydrogen to produce P4 via TS12 with a higher energy barrier of 430.1 kJ mol^{-1}. Product P4 is actually an epoxy structure where the Si–O bond lengths are 0.1682 and 0.1640 nm and the Si–O-Si bond angle is 112.7°. This species could be regarded as one of the precursors of silicon oxides, the products of SiC oxidation [22–25]. The reaction is exothermic by 181.1 kJ mol^{-1} with respect to the original reactants Si-SiC(001) + H$_2$O.

Fig. 3 Scheme and potential energy ($U_{0 K}$ in kJ mol^{-1}) profiles of the reactions between H_2O and the Si-terminated SiC surface obtained with ONIOM(CASSCF(5,5)/6-311G(d,p):AM1:UFF) method. **a** The overall scheme of the reaction paths, **b** the potential energy profiles of the reactions
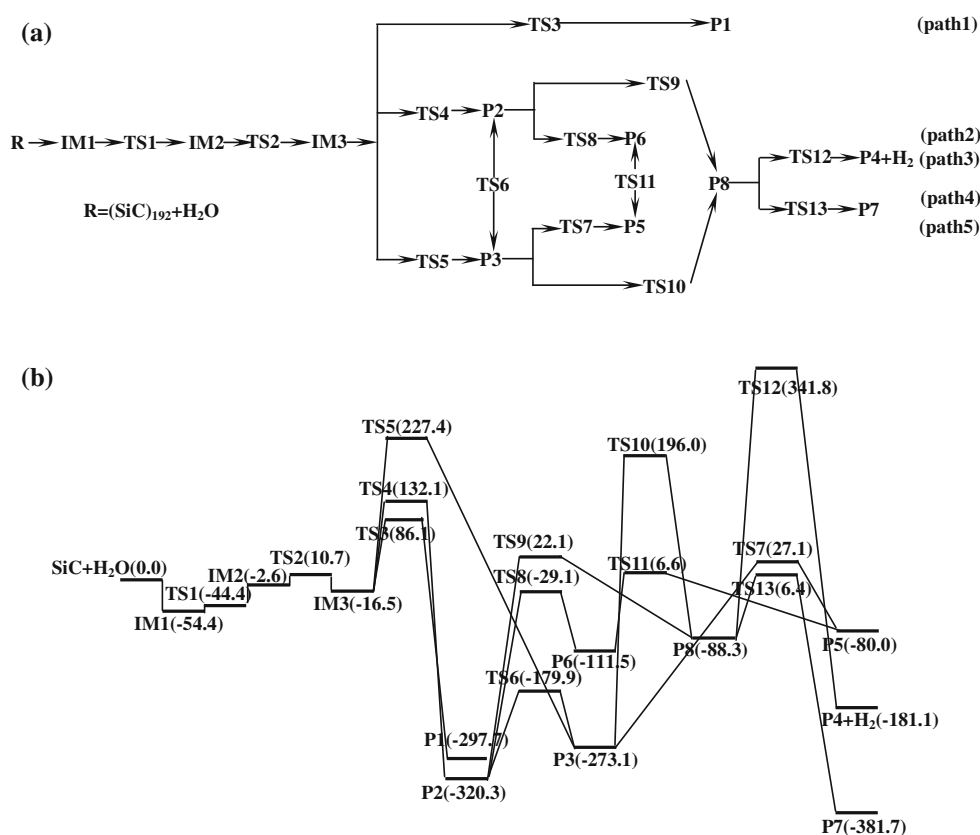
Product P8 would also isomerize into product P7 via TS13 by shifting the hydrogen atom from the hydroxyl group to the nearest unsaturated Si as shown in Fig. 2. This process has an energy barrier of 94.7 kJ mol^{-1} accompanied with 293.4 kJ mol^{-1} of heat releasing. In P7, the O atom has inserted into the H-passivated silicon atoms and a homogeneous H–Si–O–Si–H structure on the surface is formed. It is possible that the surface may become complete inertia if all the dangling bonds are terminated by hydrogen atoms in the similar pattern.

The necessary energy barriers to produce P1, P2, P3, P5 and P6 are relatively lower by 102.6 kJ mol^{-1} for P1, 148.6 kJ mol^{-1} for P2 and P3, and 291.2 kJ mol^{-1} for P5 and P6. These reactions are considered feasible at higher temperatures. Thus, the main products are P1, P2, P3, P5 and P6, among which, the production of P1 has the lowest barrier of 102.6 kJ mol^{-1} and P2 is the most stable species that has the largest exothermic reaction energy of 320.3 kJ mol^{-1}. Though P7 is the most stable species that has the largest exothermic reaction energy of 381.7 kJ mol^{-1}, the production of P7 is less competitive due to the higher energy barrier in TS9 by 342.4 kJ mol^{-1} or TS10 by 469.1 kJ mol^{-1}.

It should be interesting to compare the results with those on the C-terminated surface [1]. Firstly, the interaction of the water molecule with the Si-terminated surface should be in the triplet state rather than in the singlet state.

Secondly, the lowest energy barrier in producing P1 is 102.6 kJ mol^{-1} compared with 125.8 kJ mol^{-1} for producing the C-P5 on the C-terminated surface [1]. Thirdly, there are five main products on the Si-terminated surface compared with three on the C-terminated surface. For producing the similar products P2 and P3 (as P3 and P6 in [1]), the energy barrier, 148.6 kJ mol^{-1}, is similar by 163.8 kJ mol^{-1} for the C-P3 and 141.6 kJ mol^{-1} for the C-P6. Finally, the reaction energies for producing two stable species P2 and P7 are -320.3 and -381.7 kJ mol^{-1} on the Si-terminated surface, and those for the other two most stable products C-P3 and C-P6 are -123.7 and -138.0 kJ mol^{-1} on the C-terminated surface [1].

4 Conclusions

The reactivity of H_2O molecule on the Si-terminated silicon carbide (SiC) surface was investigated with the combined first principle and molecular mechanics method ONIOM(CASSCF:AM1:UFF). It is found that all the reactants, intermediates and products in the triplet states are more stable than those in the singlet states. A H_2O molecule and the surface can form a stronger (-54.4 kJ mol^{-1}) physically absorbed complex (IM1), and the complex can transform into other two (IM2 and IM3) complexes with very small energy barriers. For the further dissociations,

five reaction paths are found. Among which, products P1, P2, P3, P5 and P6 are the main products kinetically with the highest energy barriers of 102.6 kJ mol^{-1} for P1, 148.6 kJ mol^{-1} for P2 and P3, and 291.2 kJ mol^{-1} for P5 and P6. P4, P7 and P8 are the minor products due to the necessary energy barriers of higher than 300.0 kJ mol^{-1}. Compared with the interaction with the C-terminated surface, the H_2O interaction with the Si-terminated surface has reactions on the triplet state potential energy surface, stronger physisorption energy, smaller lowest necessary energy barrier, more main products and more stable products.

References

1. Liu Y, Su KH, Wang X, Wang YL, Zeng QF, Cheng LF, Zhang LT (2010) Chem Phys Lett 501:87
2. Cicero G, Galli G, Catellani A (2004) J Phys Chem B 108:16518
3. Cicero G, Galli G, Catellani A (2004) Phys Rev Lett 93:016102/1
4. Wang JJ, Zhang LT, Zeng QF, Vignoles LG, Guette A (2009) Chin Sci Bull 54:1487
5. Wang JJ, Zhang LT, Zeng QF, Vignoles LG, Cheng LF, Guette A (2009) Phys Rev B 79:125304/1
6. Maeda M, Nakamura K, Ohkubo T (1988) J Mater Sci 23:3933
7. Wang JJ, Zhang LT, Zeng QF, Vignoles LG, Guette A (2008) J Am Ceram Soc 91:1665
8. Bermudez VM (1989) J Appl Phys 66:6084
9. Bermudez VM (1995) Appl Sur Sci 84:45
10. Amy F, Chabal YJ (2003) J Chem Phys 119:6201
11. Ventra MD, Pantelides ST (1999) Phys Rev Lett 83:1624
12. Wu SJ, Cheng LF, Zhang LT, Xu YD, Zhang Q (2006) Mater Sci Eng B 130:215
13. Fukushima M, Zhou Y, Yoshizawa YI, Hirao K (2008) J Eur Ceram Soc 28:1043
14. Okawa T, Fukuyama R, Hoshino Y, Nishimura T, Kido Y (2007) Sur Sci 601:706
15. Voegeli W, Akimoto K, Urata T, Nakatani S, Sumitani K, Takahashi T, Hisada Y, Mitsuoka Y, Mukainakano S, Suguyama H, Zhang XW, Kawata H (2007) Sur Sci 601:1048
16. Hoshino Y, Okawa T, Shibuya M, Nishimura T, Kido Y (2008) Sur Sci 602:3253
17. Li SW, Feng ZD, Mei H, Zhang LT (2008) Mater Sci Eng A 487:424
18. Liu CD, Cheng LF, Mei H, Luan XG (2009) Ceram Int 35:1397
19. Yin XW, Cheng LF, Zhang LT, Xu YD (2003) Mater Sci Eng A 348:47
20. Eaton HE, Linsey GD (2002) J Eur Ceram Soc 22:2741
21. Irene EA, Ghez R (1977) J Electrochem Soc 124:1757
22. Opila EJ (1999) J Am Ceram Soc 82:625
23. Opila EJ Jr, Hann RE (1997) J Am Ceram Soc 80:197
24. Opila EJ, Fox DS, Jacobson NS (1997) J Am Ceram Soc 80:1009
25. Opila EJ, Smialek JL, Robinson RC, Fox DS, Jacobson NS (1999) J Am Ceram Soc 82:1826
26. Dapprich S, Komáromi I, Byun KS, Morokuma K, Frisch MJ (1999) J Mol Struct (Theochem) 461–462:1
27. Svensson M, Humbel S, Froese RDJ, Matsubara T, Sieber S, Morokum K (1996) J Phys Chem 100:19357
28. Svensson M, Humbel S, Morokuma K (1996) J Chem Phys 105:3654
29. Tamura H, Gordon MS (2003) J Chem Phys 119:10318
30. Hegarty D, Robb MA (1979) Mol Phys 38:1795
31. Eade RHA, Robb MA (1981) Chem Phys Lett 83:362
32. Schlegel HB, Robb MA (1982) Chem Phys Lett 93:43
33. Bernardi F, Bottini A, McDougall JJW, Robb MA, Schlegel HB (1984) Far Symp Chem Soc 19:137
34. Yamamoto N, Vreven T, Robb MA, Frisch MJ, Schlegel HB (1996) Chem Phys Lett 250:373
35. Frisch MJ, Ragazos IN, Robb MA, Schlegel HB (1992) Chem Phys Lett 189:524
36. Dewar M, Thiel W (1977) J Am Chem Soc 99:4499
37. Dewar MJS, McKee ML, Rzepa HS (1978) J Am Chem Soc 100:3607
38. Dewar MJS, Zoebisch EG, Healy EF (1985) J Am Chem Soc 107:3902
39. Rappé AK, Casewit CJ, Colwell KS, Goddard WA III, Skiff WM (1992) J Am Chem Soc 114:10024
40. Maseras F, Morokuma K (1995) J Comput Chem 16:1170
41. Frisch MJ, Trucks GW, Schlegel HB, Scuseria GE, Robb MA, Cheeseman JR, Scalmani G, Barone V, Mennucci B, Petersson GA, Nakatsuji H, Caricato M, Li X, Hratchian HP, Izmaylov AF, Bloino J, Zheng G, Sonnenberg JL, Hada M, Ehara M, Toyota K, Fukuda R, Hasegawa J, Ishida M, Nakajima T, Honda Y, Kitao O, Nakai H, Vreven T, Montgomery JA Jr, Peralta JE, Ogliaro F, Bearpark M, Heyd JJ, Brothers E, Kudin KN, Staroverov VN, Kobayashi R, Normand J, Raghavachari K, Rendell A, Burant JC, Iyengar SS, Tomasi J, Cossi M, Rega N, Millam JM, Klene M, Knox JE, Cross JB, Bakken V, Adamo C, Jaramillo J, Gomperts R, Stratmann RE, Yazyev O, Austin AJ, Cammi R, Pomelli C, Ochterski JW, Martin RL, Morokuma K, Zakrzewski VG, Voth GA, Salvador P, Dannenberg JJ, Dapprich S, Daniels AD, Farkas O, Foresman JB, Ortiz JV, Cioslowsk J, Fox DJ (2009) Gaussian 09, Revision A.02, Gaussian Inc., Wallingford, CT
42. Pollmann J, Kruger P (2004) J Phys Condens Matt 16:S1659
43. Powers JM, Wander A, Van Hove MA, Somorjai GA (1992) Surf Sci Lett 260:L7
44. Foster JP, Weinhold F (1980) J Am Chem Soc 102:7211
45. Reed AE, Weinstock RB, Weinhold F (1985) J Chem Phys 83:735